Materials Science and Engineering C 32 (2012) 1247–1252

Contents lists available at SciVerse ScienceDirect

Materials Science and Engineering C

journal homepage: www.elsevier.com/locate/msec

Carbon nanomaterials as drug carriers: Real time drug release investigation

Renyun Zhang *, Håkan Olin *

Department of Natural Sciences, Engineering and Mathematics, Mid Sweden University, SE 851 70 Sundsvall, Sweden

ARTICLE INFO

Article history:
Received 10 July 2011
Received in revised form 6 January 2012
Accepted 24 March 2012
Available online 30 March 2012

Keywords:
Drug release
Carbon black
Carbon nanotube
Graphene oxide
pH influence

ABSTRACT

The use of carbon nanomaterials in biomedical applications and the cytotoxicity of these materials have been areas of great interest during the last decade. In vitro drug load and release, as well as in vivo animal tests, have been carried out using carbon nanomaterials. However, no comparison studies on the drug load and the release of different carbon nanomaterials have been reported. Here, we report on a real time investigation of the drug release of carbon black (CB) nanoparticles, carbon nanotubes (CNTs) and graphene oxide (GO), using rhodamine B (RB) as a model of drug. The binding of RB to the nanomaterials were characterized by FTIR and UV–vis. The mass loading capacities of these nanomaterials were also studied, showing that GO had the highest capacity. The real time drug release experiment indicated different accumulative release modes of these nanomaterials at different pH values, due to their different binding modes with RB, which is also discussed as being the reason for the mechanism differences. Moreover, the comparison of the drug release capacity of CNT–RB and *f*-CNT–RB (functionalized-CNT–RB) indicated an influence of hydrogen bonds in both drug loading and release, as the hydrogen bonds increased the loading capacity of the carbon nanotube after acid treatment and changed the drug release mechanism at pH 7.4. Thus, here we identified the drug release modes of the different carbon nanomaterials. The results of the influence of functional groups and hydrogen bonds point also out a potential way of controlling the drug release behavior of carbon nanomaterials by surface modification.

1. Introduction

The current intense research on the application of nanomaterials in drug delivery shows new strategies for human healthcare. The chemical and physical properties of nanomaterials have made the researcher's attention turn also to biomedical possibilities. The surface properties of nanomaterials, such as easy modification and functionalization, make them attractive as drug carriers. The structure of the material, e.g. a porous structure, is also interesting in this context. The physical properties, like the magnetism of iron oxide nanoparticles, can also offer extra control in addition to drug delivery [1]. For example, the magnetism of iron oxide nanoparticles can be used to concentrate the magnetic nanoparticles at the target location. It can also be used to kill mutated cells by heating the nanoparticles under alternating magnetic fields [2].

Biocompatible and biodegradable nanostructures with a high drug loading capacity and a controllable drug release process are desired for biomedical applications, and extra controllable properties, like magnetism, could be added. But, in reality, it is not that easy to synthesize such nanostructures with all the desired properties, as these properties are not likely to be found in the same nanostructure. Thus, different nanostructures are developed or applied in drug delivery with different purposes.

Liposomes are attractive drug delivery systems [3]. Lipids like phospholipids in liposome bilayer have excellent biocompatibility and biodegradability, as well as high capacity for drug load. Polymer nanostructure in the form of micelles [4] are also good choices for drug delivery, since many polymers are biocompatible and biodegradable [5]. Inorganic nanoparticles, like magnetic nanoparticles [1,6–10], Au nanoparticles [11,12], silica nanoparticles [13], etc. have also proved to be useful in drug delivery.

Carbon nanomaterials are recently used in various drug release studies due to their specific structures, like the hollow structure of nanohorns, or the six-membered carbon ring in carbon nanotube and graphene. Carbon nanohorns are able to act as drug carrier using both the large surface area [14] and the hollow structures [15]. Another zero-dimensional structure, carbon nanoparticles, are used in drug delivery studies in combination with magnetic doped ones, where the carbon nanoparticle is synthesized by carbonizing polypyrrole nanoparticles [16]. Carbon black nanoparticles were recently demonstrated in use to deliver drugs, proteins and DNA into different cells while maintaining high cell viability [17]. Carbon nanotubes, a one-dimensional carbon nanostructure, have also been applied for drug discovery. For example, double functionalized carbon nanotubes by 1,3-dipolar cycloaddition of azomethine is used as a drug carrier [18]. Dai's group studied the drug loading and delivery of water-soluble carbon nanotubes, showing high load capacity [19]. His group has also investigated the drug loading and release on graphene oxide [20,21], illustrating the high drug load capacity of graphene oxide that is also found in other reports [22,23].

* Corresponding authors. Fax: +46 60 148484.
E-mail address: renyun.zhang@miun.se (R.Y. Zhang).

0928-4931/$ – see front matter © 2012 Elsevier B.V. All rights reserved.
doi:10.1016/j.msec.2012.03.016

Though the research on drug delivery using carbon nanomaterials is promising, a drug release model study is still missing, especially the comparison of the carbon nanomaterials, e.g. carbon nanoparticles and nanohorns, carbon nanotubes, and graphene or graphene oxide. Although these materials with different dimensions have different surface chemistry and crystal structures, a comparison study may give information on the structure induced drug release behavior. Besides, we lack real time in vitro measurements of these carbon nanomaterials to compare the drug release mechanisms.

In this paper, we report on a real time in vitro method to study the drug release of carbon black (CB), carbon nanotubes (CNTs) and graphene oxides (GO). The drug release mechanisms have been investigated at different pH values, showing the influence of pH on the drug release processes. Moreover, the influence of surface groups that can form hydrogen bonds was studied by comparing the drug load and release on CNT and *f*-CNT, showing the effect of hydrogen bonds. The study demonstrated the drug release behaviors of different carbon nanomaterials due to their specific structures and surface properties, which could be applied for future drug delivery research using carbon nanomaterials, for example the surface modification of carbon nanostructures like the oxygen-containing groups on graphene oxide that can be used to control the drug release under different conditions.

2. Experiment

2.1. Materials

Multi-walled carbon nanotubes with an average diameter of 140 nm were purchased from Sigma without further purification. Graphene oxide was synthesized using a modified Hummers method [24,25] from graphite (Sigma). Carbon black was purchased from Sigma without further purification and rhodamine B was purchased from Sigma. All other reagents were all of analytical grade.

2.2. Loading of RB on carbon nanomaterials

Loading of RB on CB (10 mg), CNT (10 mg) and GO (10 mg) was done by mixing a certain amount of the above materials into 8.0 ml 160 mg/l RB solution for 20 h with weak sonication. After that, the samples were kept for 4 h, then collected and centrifuged at 4000 rpm for 5 min and subsequently rinsed with doubly distilled water three times. Finally, the collected samples were re-dispersed in 150 μl double distilled water before use. The loading capacities of RB on these nanomaterials were measured with UV–vis, and were measured by calculating the loss of RB after the loading procedure, compared with the original solution.

2.3. Release of RB at different pH

Drug release experiments of RB from these three nanomaterials were done using real time monitoring method [26]. In brief, 30 μl of each sample was dropped on an Al foil plate with an area of 6 mm × 6 mm and dried at room temperature. Then the plate was put into the bottom of a cuvette and 3 ml at pH 4.5 or pH 7.4 PBS was added. pH 4.5 was selected to show the drug release of RB at an acidic environment, because some parts of the human body like the stomach and intestine are acidic, which makes the investigation at this pH reasonable. The transmittance measurements at 554 nm were performed on each sample for 20 h. All experiments were repeated at least three times.

2.4. Characterizations

FTIR experiments were performed on a Nicolet 6700 (THERMO) spectrometer to observe the transmittance of CB, CNT and GO before and after loading with RB. The UV–vis was carried out on a Lambda Bio 20 spectrometer (Perkin Elmer). The absorbance of 100 μl of the original solution or the liquid residues from the centrifuge process in 3.0 ml double distilled water was measured. Also, UV–vis was used to monitor the real time drug release behaviors of the carbon nanomaterials as described in Section 2.3.

3. Results and discussion

3.1. Loading capacity

Carbon black (CB), carbon nanotubes (CNTs) and graphene oxide (GO) are three different carbon nanomaterials with different structures. CB has an amorphous structure; CNT has a tube structure with a surface structure like graphene; GO has a flat structure, which contains –OH and –COOH groups in the flat area and at the edges. The structure differences might be the most important factor in the loading of RB.

In our experiment, the loading capacities of carbon black, carbon nanotube and graphene oxide were characterized by UV–vis. After the centrifuge separation, both solid samples and liquid residues were collected. The liquid residues were then measured by UV–vis to observe the absorbance of RB (Fig. 1). By comparing the absorbance value of the residues with the original RB solution, we were able to calculate the loading capacities of these carbon nanomaterials, which were 0.12, 0.02 and 0.09 mg for GO, CNT and CB respectively. The low loading capacity of carbon nanotubes is due to the large diameter of the CNT that we used in this study, which offered only a small surface area per unit weight, compared to single-walled carbon nanotubes.

Fig. 1 indicates that the loading capacities of these nanomaterials were different, which may be related to the surface structure of these carbon nanomaterials. GO, being plane sheets, have two sides to be loaded with RB through π–π stacking. The –OH and –COOH groups should increase the binding of GO to RB through hydrogen bonds and by electrostatic interaction, leading to higher load efficiency. Unlike GO, CNTs only have a graphene-structured surface but no –OH and –COOH groups, which is the reason that there is only a hydrophobic (including π–π stacking) interaction between RB and CNT. For CB, physical adsorption mainly contributes to the binding of RB to CB due to the amorphous structure. Since the CNT we used here is a multiwalled carbon nanotube with an average diameter of 140 nm (Sigma), the surface area is much smaller than for single-walled carbon nanotubes with the same weight. Thus, the loading capacity of RB was found to be much less. But, since we were mainly focusing on the release behavior of RB, and the loading capacity was not directly related to the release behavior, the low loading capacity of CNT here did not influence our conclusions. Fig. 2 shows a schematic

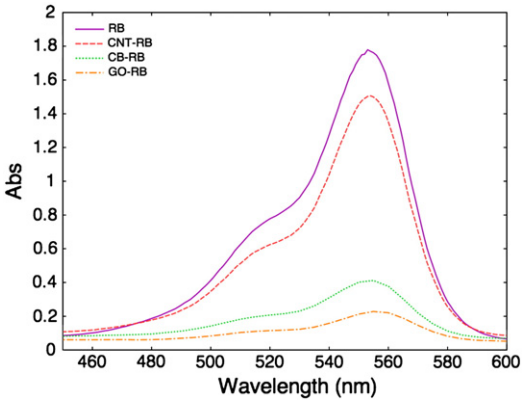

Fig. 1. UV–vis of the original rhodamine (RB) and RB residue after removal of loaded carbon black (CB), carbon nanotubes (CNTs), and graphene oxide (GO) from the RB solution.

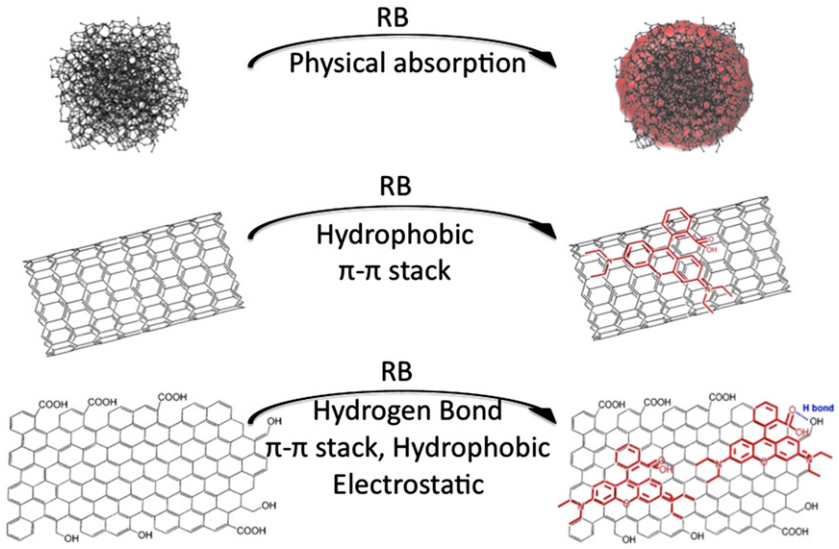

Fig. 2. Schematic drawing of the interaction of RB with CB, CNT and GO.

drawing of the possible interaction of RB with GO, CNT and CB. The CB we used in our experiments has a uniform amorphous structure, and the CNT and GO have uniform surface structures. These uniform structures lead to equal chances for RB to bind to any place of these nanomaterials, resulting in an evenly distributed RB on these materials. However, to define the distribution in detail, more experimental investigation is needed.

Apart from the liquid residues, the sediments from the centrifuge separation, and the carbon nanomaterial–RB hybrids, were also characterized, using FTIR methods. Fig. 3 shows the FTIR of the CB, CNT and GO before and after loading with RB. The bands at 1586, 1331 and 1174 cm^{-1}, correspond to the C–N and N–H bonds, the amide III, and the C–O bond of RB respectively [27]. The carbon nanomaterials were rinsed after loading, which means that these bands are from RB, indicating the successful loading of RB on these carbon materials.

3.2. Real time drug release

The release behavior of the drug from drug loaded nanomaterials is commonly pH-dependent, especially when the interaction forces of the drug and the nanomaterials are based on hydrogen bonds. For example, the strength of hydrogen bonds between –OH and –COOH groups is strongly pH value related [22]. We investigated the release behavior of RB from carbon nanomaterials at pH 4.5 and pH 7.4. To describe the drug release mechanism the following model is commonly used [28,29]:

$$\frac{Mt}{M_\infty} = kt^n, \tag{1}$$

where M_t and M_∞ are the cumulative amount of the drug released at time t and at infinite time, respectively, k is a constant incorporating structural and geometric characteristics of the drug system, and n is the diffusional exponent which is indicative of the transport mechanism of drug release. The three carbon materials have different and unknown surface areas which are included in the constant k [30] but the exponent n is independent of this area, and we can thus get information about the material dependent release rate by the value of n, by fitting the real time drug release curves with Eq. (1).

Carbon black is an amorphous carbon nanomaterial. The amorphous structure inhibits interactions with RB through π–π stacking or through hydrogen bonds, due to the lack of functional groups that can form hydrogen bonds.

The real time release result of RB from CB–RB is shown in Fig. 4. By plotting the real time release curves, the values of n were calculated as 0.32 at pH 4.5 and 0.39 at pH 7.4, indicating that a Fickian diffusion of RB from carbon black applies at both pH conditions. Fickian diffusion has usually an n value close to 0.5, however when the particle sizes are not uniform or the particles aggregate, the n value will be smaller than for monodispersed particles [29]. In our case, the CB particles were aggregated but not monodispersed, and the sizes of the aggregates were not uniform, causing the small n values of 0.32 and 0.39. Moreover, the release speed of RB at pH 4.5 was found to be higher than at pH 7.4. This might contribute to the increased solubility of RB at pH 4.5 [19,31], which causes a faster release speed of RB from CB.

Unlike the release from CB–RB hybrids, the release behavior of RB from CNT–RB showed different diffusion mechanisms at different pH values. Fig. 5 shows the real time data of the release processes at pH 4.5 and pH 7.4. At pH 7.4, the Fickian diffusion was found to be the main diffusion process, while the process changed to an anomalous transport at pH 4.5. It should be pointed out that the fit of real time release of RB at pH 4.5 (Fig. 5) was only done for the first 3 h, similar to the report by Guo et al. [32]. After this time the system was saturated and reached the maximum value and to make a proper fit it should be excluded, but the data was recorded even after saturation (and shown in Fig. 5) to keep the same monitoring time range as in the other experiments. A similar fit for the release of RB on GO at pH 7.4 was done for the data shown in Fig. 6. As mentioned above, RB was physically adsorbed on CB and thus the pH value only influences the solubility of RB. But in the case of CNT, the situation was different, since the RB could interact with CNT through hydrophobic interactions (including π–π stacking) [33]. These interactions may also be influenced by the pH value. A low pH value of 4.5 may increase the hydrophilicity and solubility of RB [19], causing the anomalous diffusion behavior. On the other hand, no such influence was observed at pH 7.4.

Compared to CNT, GO offers more chances to interact with RB apart from the hydrophobic force (including π–π stacking), because GO contains –OH and –COOH groups that can form hydrogen bonds with RB. Moreover, the –COOH group shows changes at different pH values, which generates an electrostatic interaction between GO and RB, influencing the loading and releasing of RB from GO. All these bonds and interactions should cause a higher loading capacity of GO than CNT, as described above. Also, these interactions and bonds might influence the release behavior of RB, which has been previously

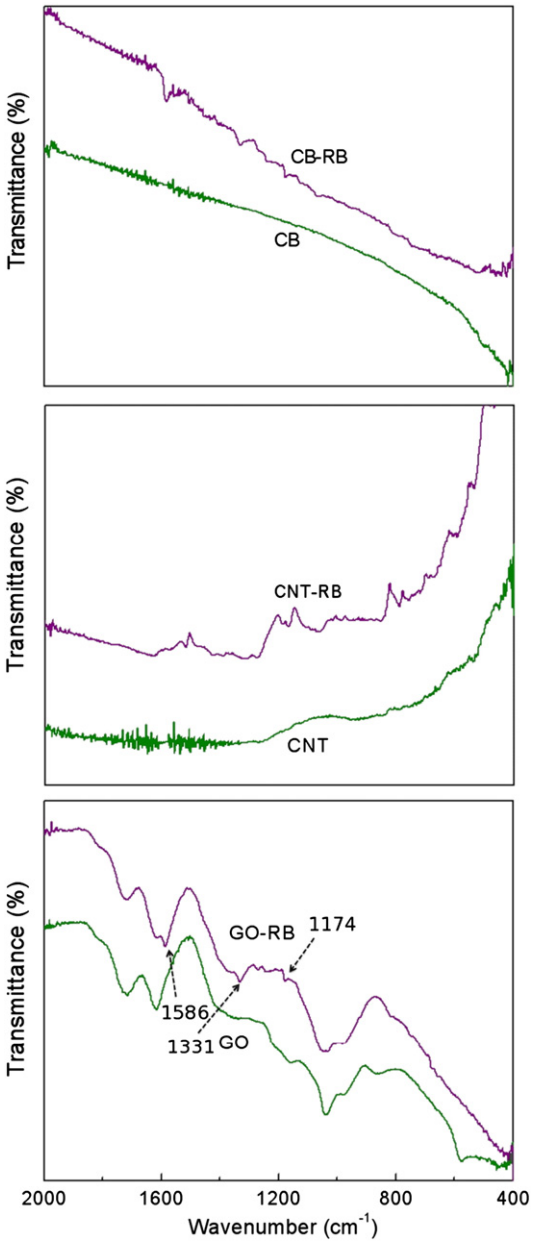

Fig. 3. FTIR of CB, CNT and GO before and after loading with RB.

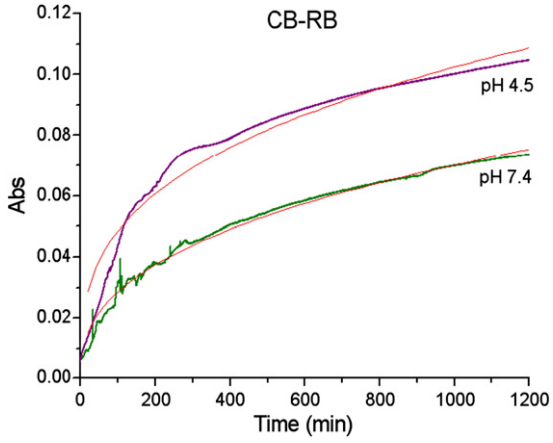

Fig. 4. Real time monitoring of the release of RB from CB at pH 4.5 and pH 7.4. The red lines show the plotting results using Eq. (1).

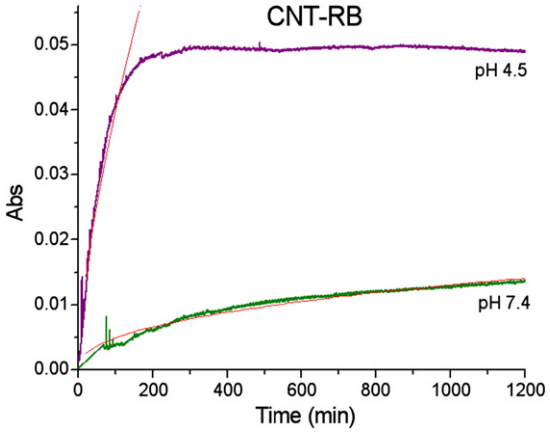

Fig. 5. Real time monitoring of the release of RB from CNT at pH 4.5 and pH 7.4. The thin red lines are plots of Eq. (1).

discussed in other contexts [26,22]. Due to these factors, the release behavior of RB from GO at different pH should be different from that of CB and CNT. In Fig. 6 a high-speed diffusion process is shown at pH 7.4, indicating a case II transport process. At pH 4.5, the hydrogen bonds are stronger than at pH 7.4 and also the hydrophobic force is stronger [34], which should reduce the diffusion speed of RB from GO. An anomalous diffusion process was found at pH 4.5.

Table 1 lists the experimental results of the three carbon nanomaterials. The same diffusion process was found for CB at both pH 4.5 and pH 7.4, while different processes were found for CNT and GO. For CB, no additional interaction besides physical adsorption, which was not influenced by the pH value, was found. The difference in release speed between the pH values is merely due to the solubility difference of RB in these two pH environments [31]. In the case of CNT, hydrophobic interactions (including π–π staking) should be the main loading mechanism of RB. At pH 4.5, the higher degree of hydrophilicity and higher solubility of RB should then explain the higher release speed compared with the case at pH 7.4 [19]. The higher release speed found at pH 4.5 in the case of CB and CNT, and lower for GO, is likely to be an effect of hydrophobic forces, hydrogen bonds and possibly by electrostatic interaction [26], resulting in a case II (relaxation controlled) transport release behavior [29].

To find whether the surface groups influenced the release behavior of RB, additional experiments should be done; for example regarding the drug release differences between graphene and graphene oxide.

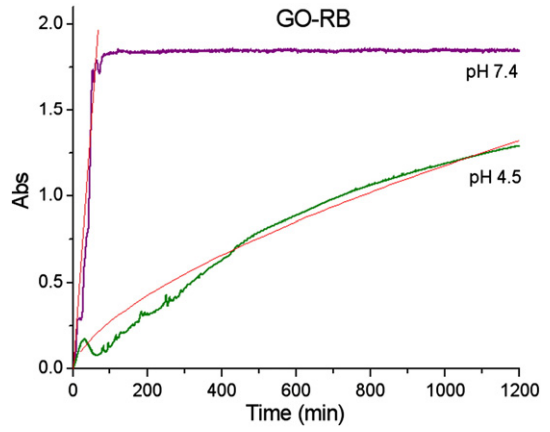

Fig. 6. Real time monitoring of the release of RB from GO at pH 4.5 and pH 7.4. The red lines are plots of Eq. (1) for $n = 0.63$ (pH 4.5) and $n = 1$ (pH 7.4).

Table 1
Plotted *n* value of the release of RB from carbon nanomaterials at pH 7.4 and pH 4.5.

	n value at pH 7.4	*n* value at pH 4.5	Drug release mode
CB–RB	0.39	0.32	Fickian diffusion
CNT–RB	0.42	0.64	Fickian diffusion at pH 7.4, anomalous transport at pH 4.5
f-CNT–RB	0.5	0.64	Anomalous transport
GO–RB	1	0.63	Case II transport at pH7.4, anomalous transport at pH 4.5

But, since it is not easy to get a bulk amount of graphene with a perfect surface structure (graphene reduced from GO has defects on the surface), we choose CNT instead. A comparison experiment was made between CNT and *f*-CNT, where the *f*-CNT was acid treated CNT (H_2SO_4: HNO_3, 3:1) that generates –OH and –COOH groups on carbon nanotubes. The comparison showed that the loading capacity of *f*-CNT was 3.5 times higher than that of CNT (Fig. 7A), indicating the assistance of hydrogen bonds to the loading of RB to *f*-CNT and GO surfaces. Also, the release behavior of RB from *f*-CNT was not the same as from CNT.

Fig. 7B shows the real time monitoring of the drug release of *f*-CNT–RB at pH 4.5 and pH 7.4. Fitting Eq. (1) to the experimental data indicated that the *n* value was still 0.64 at pH 4.5, which pointed toward an anomalous diffusion. However, the release behavior of RB at pH 7.4 was different from CNT–RB, and the *n* value was 0.5. The *n* value at pH 7.4 indicated an anomalous diffusion of RB from *f*-CNT–RB, while it was a Fickian diffusion for CNT–RB (Table 1).

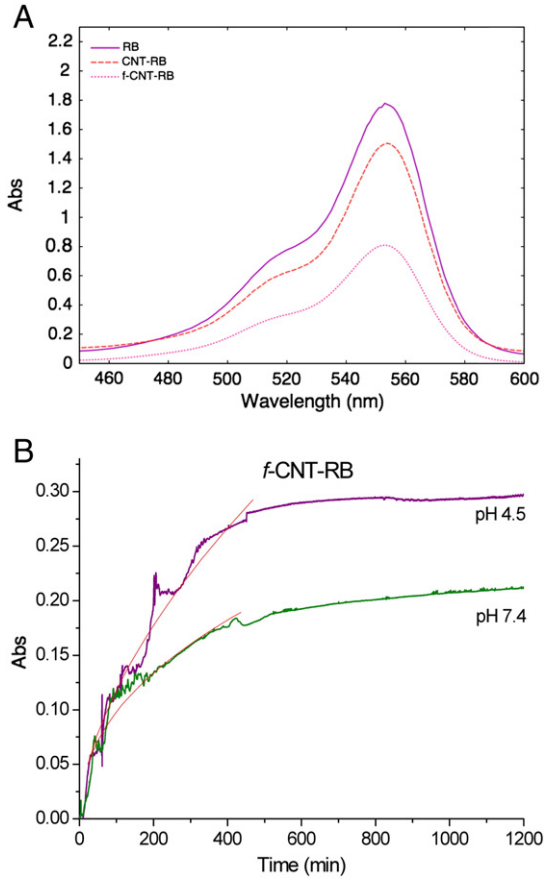

Fig. 7. (A) UV–vis of original RB, and RB residue after removal of loaded CNT and *f*-CNT from the RB solution. (B) Real time drug release of *f*-CNT–RB for 20 h. Red lines in (B) are from the model described by Eq. (1).

In this study, the difference between *f*-CNT and CNT was the –OH and –COOH groups that were generated by acid treatment. Regarding binding, *f*-CNT offered hydrogen bonds that were not offered by CNT, which increased the loading capacity as described above. If we compare the drug release of CNT–RB with *f*-CNT–RB at pH 7.4, the diffusion mode changed from a Fickian diffusion to an anomalous diffusion, which could be contributed by the hydrogen bonds as discussed in the GO–RB release [26]. This result suggests that the drug release behavior can be controlled by changing the surface groups of carbon nanomaterials. This may be used to control the drug delivery mode and its speed in experimental and real applications.

4. Conclusions

In summary, we investigated load and real time release of RB on three carbon nanomaterials: carbon black (CB), carbon nanotubes (CNTs) and graphene oxide (GO). GO was found to have the highest loading capacity, while CNT had the lowest, which was due to the smaller surface area and lack of functional groups. The release behavior of RB turned out to be pH dependent. The pH value influenced the interaction affinities between RB and these carbon materials, where the affinities depended on the surface chemistry. The results indicated that the Fickian diffusion was the main process for the release of RB from CB–RB at the studied pH values, while the release modes were different for RB from CNT–RB and GO–RB at different pH values. Anomalous diffusion was found at pH 4.5 for both CNT–RB and GO–RB, while it was a Fickian transport for CNT–RB and a Case II transport for GO–RB at pH 7.4. The different behaviors of GO–RB may be influenced by the hydrogen bonds between GO and RB at different pH values. Since it is not easy to get a bulk amount of graphene with a perfect surface, we used *f*-CNT instead, to confirm the influence of hydrogen bonds, suggesting controllable drug release by changing the surface structure of carbon nanomaterials.

Acknowledgment

We thank Sundsvall Community for the financial support.

References

[1] R.Y. Zhang, X.M. Wang, C.H. Wu, M. Song, J.Y. Li, G. Lv, J. Zhou, C. Chen, Y.Y. Dai, F. Gao, D.G. Fu, X.M. Li, Z.Q. Guan, B.A. Chen, Nanotechnology 17 (2005) 3622–3626.
[2] R. Ivkov, S.J. DeNardo, W. Daum, A.R. Foreman, R.C. Goldstein, V.S. Nemkov, G.L. DeNardo, Clin. Cancer Res. 11 (2005) 7093s–7102s.
[3] Y. Malam, M. Loizidou, A.M. Seifalian, Trends Pharmarcol. Sci. 30 (2009) 592–599.
[4] S. Cammas, K. Suzuki, C. Sone, Y. Sakurai, K. Kataoka, T. Okano, J. Control. Release 48 (1997) 157–164.
[5] Y. Lu, S.C. Chen, Adv. Drug Delivery Rev. 56 (2004) 1621–1633.
[6] R.Y. Zhang, C.H. Wu, X.M. Wang, Q. Sun, B.A. Chen, X.M. Li, S. Gutmann, G. Lv, Mater. Sci. Eng. C 5 (2009) 1697–1701.
[7] X.M. Wang, R.Y. Zhang, C.H. Wu, Y.Y. Dai, M. Song, S. Gutmann, F. Gao, G. Lv, J.Y. Li, X.M. Li, Z.Q. Guan, D.G. Fu, B.A. Chen, J. Biomed. Mater. Res. A 80A (2006) 852–860.
[8] M. Arruebo, R. Fernandez-Pacheco, M.R. Ibarra, J. Santamaria, Nano Today 3 (2007) 22–32.
[9] T.K. Jian, J. Richey, M. Strand, D.L. Leslie-Pelecky, C.A. Flask, V. Labhasetwar, Biomaterials 29 (2008) 4012–4021.
[10] C. Alexiou, W. Arnold, R.J. Klein, F.G. Parak, P. Hulin, C. Bergemann, W. Erhardt, S. Wagenpfeil, A.S. Lubbe, Cancer Res. 60 (2000) 6641–6648.
[11] G.F. Paciotti, L. Myer, D. Weinreich, D. Goia, N. Pavel, E.R. McLaughlin, L. Tamarkin, Drug Deliv. 11 (2004) 169–183.
[12] P. Ghosh, G. Han, M. De, C.K. Kim, V.M. Rotello, Adv. Drug Deliv. Rev. 60 (2008) 1307–1315.
[13] Y.N. Zha, B.G. Trewyn, I.I. Slowing, V.S.Y. Lin, J. Am. Chem. Soc. 131 (2009) 8398–8400.
[14] T. Murakami, K. Ajima, J. Miyawaki, M. Yudasaka, S. Iijima, K. Shiba, Mol. Pharm. 1 (2004) 399–405.
[15] K. Ajima, M. Yudasaka, T. Murakami, A. Maigne, K. Shiba, S. Iijima, Mol. Pharm. 2 (2005) 475–480.
[16] W.K. Oh, H. Yoon, J. Jang, Biomaterials 31 (2010) 1342–1348.
[17] P. Chakravarty, W. Qian, M.A. El-Sayed, M.R. Prausnitz, Nat. Nanotech. 5 (2010) 607–611.
[18] G. Pastorin, W. Wu, S. Wieckowski, J.-P. Briand, K. Kostarelos, M. Prato, A. Bianco, Chem. Commun. (2006) 1182–1184.

[19] Z. Liu, X.M. Sun, N. Nakayama-Ratchford, H.J. Dai, ACS Nano 1 (2007) 50–56.
[20] X.M. Sun, Z. Liu, K. Welsher, J.T. Robinson, A. Goodwin, S. Zaric, H.J. Dai, Nano Res. 1 (2008) 203–212.
[21] Z. Liu, J.T. Robinson, X.M. Sun, H.J. Dai, J. Am. Chem. Soc. 130 (2008) 10876–10877.
[22] X.Y. Yang, X.Y. Zhang, Z.F. Liu, Y.F. Ma, Y. Huang, Y.S. Chen, J. Phys. Chem. C 112 (2008) 17554–17558.
[23] L.M. Zhang, J.G. Xia, Q.H. Zhao, L.W. Liu, Z.J. Zhang, Small 6 (2009) 537–544.
[24] W.S. Hummers, R.E. Offeman, J. Am. Chem. Soc. 80 (1958) 1339-1339.
[25] M. Hirata, T. Gotou, S. Horiuchi, M. Fujiwara, M. Ohba, Carbon 42 (2004) 2929–2937.
[26] R.Y. Zhang, M. Hummelgård, G. Lv, H. Olin, Carbon 49 (2011) 1126–1132.
[27] S.K. Das, J. Bhowal, A.R. Das, A.K. Guha, Langmuir 22 (2006) 7256–7272.
[28] R.S. Langer, N.A. Peppas, Biomaterials 2 (1981) 201–214.
[29] B. Kim, K.L. Flamme, N.A. Peppas, J. Appl. Polym. Sci. 89 (2003) 1606–1613.
[30] A. Judefeind, M.M. de Villiers, in: M.M. de Villiers, P. Aramwit, G.S. Kwon (Eds.), Nanotechnology in Drug Delivery, Springer/AAP Press, New York, 2009, p. 147.
[31] R.W. Ramette, E.B. Sandell, J. Am. Chem. Soc. 78 (1956) 4872–4878.
[32] X.D. Guo, L.J. Zhang, Y. Chen, Y. Qian, AICHE J. 56 (2010) 1922–1931.
[33] I. Moreno-Villoslada, M. Jofré, V. Miranda, R. González, T. Sotelo, S. Hess, B.L. Rivas, J. Phys. Chem. B 110 (2006) 11809–11812.
[34] A. Kim, L.J. Cote, W. Yuan, K.R. Shull, J.X. Huang, J. Am. Chem. Soc. 132 (2010) 8180–8186.